Journal of Earth Science, *Vol. 29*, *No. 5*, *p. 977–988*, *October 2018* *ISSN 1674-487X*
Printed in China
https://doi.org/10.1007/s12583-018-0851-z

Metapelitic Garnet-Muscovite-Al_2SiO_5-Quartz (GMAQ) Geothermobarometry

Chun-Ming Wu*
College of Earth and Planetary Sciences, *University of Chinese Academy of Sciences*, *Beijing* 100049, *China*
Chun-Ming Wu: https://orcid.org/0000-0003-0214-6313

ABSTRACT: The garnet-muscovite geothermometer and garnet-muscovite-Al_2SiO_5-quartz (GMAQ) geobarometer have been empirically calibrated under *P-T* conditions of 1–12 kbar and 460–760 ºC using natural metapelitic rocks. The chemical compositions of the calibrant muscovite are in the ranges of Fe=0.03–0.21 atoms, Mg=0.02–0.32 atoms and Al^{VI}=1.62–1.96 atoms, respectively, on the 11-oxygen basis per formula unit. The garnet-muscovite thermometer yields similar temperature estimates to the well calibrated garnet-biotite thermometer within error of ±55 °C, and successfully discriminates the systematic temperature change of the different zones of either the prograde or inverted metamorphic terranes or thermal contact aureoles. The six formulations of GMAQ barometry yield similar pressure estimates to the well calibrated GASP barometer within error of ±1.2 kbar, and plot the Al_2SiO_5-bearing metapelite into the correct stability field of the Al_2SiO_5 polymorphs. Moreover, the GMAQ thermobarometers show that the pressure is almost constant for every thermal contact aureole within limited geographic region, which reflects geological condition. The random errors are estimated to be of ca. ±60 °C and ±1.4 kbar for the geothermometer and geobarometer, respectively. A spreadsheet for applying GMAQ geothermobarometry is supplied in the Electronic Supplementary Materials.
KEY WORDS: Al_2SiO_5, application, calibration, garnet, geothermobarometry, muscovite.

0 INTRODUCTION

It is well known that garnet-bearing metapelite is not only sensitive to temperature and/or pressure changes (e.g., Maldonado et al., 2018; Chatterjee, 2016; Chen et al., 2009, 1998; Cheng et al., 2009; Holdaway, 2001, 2000; You et al., 1993; Chen, 1990; Koziol and Newton, 1988; Spear et al., 1984; Perchuk and Lavrent'eva, 1983), but is also an ideal videocorder of deformational events (e.g., Ali et al., 2016; Zhang et al., 2012, 2009; Li et al., 2011, 2010, 2005; Bell and Mares, 1999; Johnson, 1999; Jones, 1994; Bell et al., 1992; Zwart, 1962). Therefore, garnet-bearing metapelite is the absolutely necessary target in metamorphic research, along with the garnet-bearing metamorphic mafic rocks. In determining temperature (*T*) and pressure (*P*) conditions of these metamorphic rocks, geothermometry and geobarometry play irreplaceable important roles.

There are currently two types of conventional geothermobarometers. The first kind is independently calibrated using available primary experimental and/or natural data, such as the garnet- biotite thermometer (e.g., Holdaway, 2000; Kleemann and Reinhardt, 1994; Perchuk and Lavrent'eva, 1983; Ferry and Spear, 1978) and the garnet-aluminosilicate-plagioclase-quartz (GASP) barometer (e.g., Holdaway, 2001), as well as some mono-mineralogical geothermobarometers, such as the Zr-in-rutile thermometer (Şengün and Zack, 2016; Tomkins et al., 2007) and the Ti-in-zircon thermometer (Ferry and Watson, 2007). Another type is the multiple thermobarometry method, i.e., a self-consistent thermodynamic database developed using statistical or mathematical programming methods applied to all the experimental data available for the related compositional systems (Holdaway, 2001), such as the TWQ software (Berman, 1991) and the average *P-T* method (Powell et al., 1998). However, if secondary constraints involve systematic errors in thermodynamic data and related *P-T* equilibria, it is quite possible that such multiple thermobarometry may have systematic *P-T* errors between specimens of differing compositions, between differing *P-T* conditions of formation, or between various equilibria. Because of these reasons, the *P-T* errors of such multiple thermobarometry may still be larger than for a carefully calibrated individual geothermobarometer (Holdaway, 2001).

Because the mineral assemblage and mineral chemistry of garnet-bearing metapelite are sensitive to *P-T* conditions in metamorphic events, such metapelite usually records the metamorphic history of metamorphic terranes. Therefore, a set of relatively accurate and precise geothermobarometers have been calibrated for metapelite, such as the garnet-muscovite thermometer (e.g., Wu and Zhao, 2006a; Wu et al., 2002; Hynes and Forest, 1988; Green and Hellman, 1982; Krogh and Råheim, 1978), the garnet-rutile-aluminosilicate-ilmenite-quartz (GRAIL) barometer (e.g., Bohlen et al., 1983), the garnet-biotite-muscovite-plagioclase (GBMP) barometer (Wu, 2015), the garnet-biotite-Al_2SiO_5-quartz (GBAQ) barometer (Wu, 2017) and the garnet-

*Corresponding author: wucm@ucas.ac.cn

Manuscript received April 25, 2018.
Manuscript accepted July 15, 2018.

rutile-ilmenite-plagioclase-quartz (GRIPS) barometer (e.g., Wu and Zhao, 2006b; Bohlen and Liotta, 1986). However, it is known that many metapelites are CaO-undersaturated, thus the plagioclase is accordingly CaO-deficient and sometimes plagioclase even does not exist, under such circumstances all the above plagioclase-bearing geobarometers lose their usage. Moreover, most metapelites are TiO_2-undersaturated and contain no rutile or ilmenite, thus, the alternative rutile- and/or ilmenite-related geobarometers (e.g., GRIPS, GRAIL) cannot be applied, either.

Therefore, geothermobarometers involving muscovite without plagioclase are of great interest to the metamorphic community, since many low- to medium-grade metapelites contain abundant muscovite but little or no plagioclase. In this contribution, adopting valid activity model of garnet, the garnet-muscovite geothermometer and the garnet-muscovite-aluminosilicate-quartz (GMAQ) geobarometer have been empirically calibrated. Applications of these GMAQ thermobarometers show that this thermometer-barometer pair is valid to either CaO-undersaturated or -saturated metapelite metamorphosed at the crustal level. Throughout this paper, mineral abbreviations are after Whitney and Evans (2010).

1 CALIBRATION DATA SET

In fact, the garnet-phengite thermometer has been experimentally calibrated (Green and Hellman, 1982; Krogh and Råheim, 1978) under high-*P*-*T* conditions, exceeding the *P*-*T* conditions of common metapelite formed in the crust. The GMAQ barometer has not been experimentally calibrated until today. Therefore, both the garnet-muscovite thermometer and the GMAQ barometer for crustal metapelite can only be empirically calibrated.

Empirical calibration requires natural rock samples which contain mineral assemblages formed at thermodynamic equilibrium. The criteria for selecting suitable natural metapelitic samples from the literature are as follows: (1) equilibrium textures in the samples are clearly described; (2) the samples did not undergo retrogressive metamorphism; (3) there are detailed and high quality electron microprobe analyses of the minerals involved, at least the SiO_2, TiO_2, Al_2O_3, FeO, MnO, MgO, CaO, Na_2O and K_2O contents are reported; (4) the samples plotted into the wrong stability field of the Al_2SiO_5 polymorphs were ascribed to possible disequilibrium assemblages and thus were discarded from the data set; and (5) if there is growth zoning in garnet, only the rim composition was used, and accordingly, only the (rim) compositions of the matrix minerals not in contact with garnet were used. Based on these criteria, the total 161 Al_2SiO_5-bearing metapelitic samples (see Table S1 and references therein) were selected for calibrating the thermobarometers, among which 13 samples contain andalusite, 2 samples contain andalusite and sillimanite, 39 samples contain sillimanite, 4 samples contain sillimanite and kyanite and the remaining 103 samples contain kyanite. These metapelites were metamorphosed under *P*-*T* conditions of 1–12 kbar and 460–760 ºC, respectively, determined by simultaneously applying the garnet-biotite thermometer (Holdaway, 2000) and the GASP barometer (Holdaway, 2001) as suggested by Wu and Cheng (2006). The chemical compositions of the calibrant muscovite cover more than 90% of natural metapelitic muscovite and the chemical ranges are restricted to Fe=0.03–0.21 atoms, Mg=0.02–0.32 atoms and Al^{VI}=1.62–1.96 atoms, respectively, on the 11-oxygen basis. Chemical compositions of the calibrant garnet are restricted in the compositional ranges of X_{Fe}^{Grt}=0.53–0.91, X_{Mg}^{Grt}=0.04–0.27, X_{Ca}^{Grt}=0.02–0.22, and X_{Mn}^{Grt}=0.00–0.29, respectively, which cover compositional ranges of almost all the metapelitic garnet.

2 THERMODYNAMIC BACKGROUND OF THE GMAQ THERMOBAROMETERS

2.1 Model Reactions

The garnet-muscovite Fe-Mg exchange thermometer is described as (Hynes and Forest, 1988; Green and Hellman, 1982; Krogh and Råheim, 1978)

$$\begin{aligned} &Mg_3Al_2Si_3O_{12}+3K(FeAl)Si_4O_{10}(OH)_2 = \\ &\quad \text{Pyrope} \qquad \text{Fe-celadonite} \\ &Fe_3Al_2Si_3O_{12}+3K(MgAl)Si_4O_{10}(OH)_2 \\ &\text{Almandine} \qquad \text{Mg-celadonite} \end{aligned} \tag{1}$$

The GMAQ geobarometer is based on the model reaction (Hodges and Crowley, 1985)

$$\begin{aligned} &Fe_3Al_2Si_3O_{12}+3KAl_2(AlSi_3)O_{10}(OH)_2+4SiO_2 = \\ &\text{Almandine} \qquad \text{Muscovite} \qquad \text{Quartz} \\ &3K(FeAl)Si_4O_{10}(OH)_2+4Al_2SiO_5 \\ &\quad \text{Fe-celadonite} \qquad \text{Aluminosilicate} \end{aligned} \tag{2}$$

which is designated as the Fe-endmember GMAQ model reaction.

Additionally, the author found that the equivalent Mg-endmember GMAQ model reaction

$$\begin{aligned} &Mg_3Al_2Si_3O_{12}+3KAl_2(AlSi_3)O_{10}(OH)_2 + 4SiO_2 = \\ &\quad \text{Pyrope} \qquad \text{Muscovite} \qquad \text{Quartz} \\ &3K(MgAl)Si_4O_{10}(OH)_2+4Al_2SiO_5 \\ &\quad \text{Mg-celadonite} \qquad \text{Aluminosilicate} \end{aligned} \tag{3}$$

can also be calibrated as a GMAQ geobarometer.

Thermodynamic equilibria of these thermobarometric model reactions can be described respectively as

$$\begin{aligned} \Delta_1 G=0=\Delta_1 H^0 - T\Delta_1 S^0 + (P-1)\Delta_1 V^0 + RT\ln K_{D(1)} + \\ 3RT\ln(\gamma_{\text{Mg-Cel}}^{\text{Ms}}/\gamma_{\text{Fe-Cel}}^{\text{Ms}}) + RT\ln(\gamma_{\text{alm}}^{\text{Grt}}/\gamma_{\text{prp}}^{\text{Grt}}) \end{aligned} \tag{4}$$

$$\begin{aligned} \Delta_2 G=0=\Delta_2 H^0 - T\Delta_2 S^0 + (P-1)\Delta_2 V^0 + \\ 3RT\ln(\gamma_{\text{Fe-Cel}}^{\text{Ms}}/\gamma_{\text{Ms}}^{\text{Ms}}) - RT\ln\gamma_{\text{alm}}^{\text{Grt}} + RT\ln K_{D(2)} \end{aligned} \tag{5}$$

$$\begin{aligned} \Delta_3 G=0=\Delta_3 H^0 - T\Delta_3 S^0 + (P-1)\Delta_3 V^0 + \\ 3RT\ln(\gamma_{\text{Mg-Cel}}^{\text{Ms}}/\gamma_{\text{Ms}}^{\text{Ms}}) - RT\ln\gamma_{\text{prp}}^{\text{Grt}} + RT\ln K_{D(3)} \end{aligned} \tag{6}$$

in which ΔG is Gibbs free energy of the reaction, and ΔH^0, ΔS^0 and ΔV^0 are the enthalpic, entropic and volumetric changes of the reaction at the P and T of interest, respectively. The γ_j^i denotes the activity coefficient of phase component j in mineral i. It has been assumed that the Al_2SiO_5 polymorphs and quartz are pure phases, and heat capacity, thermal expansion and compressibility coefficients of the phases involved have also been neglected in the *P*-*T* ranges of the crustal level. The molar fractions of the phase components of garnet and muscovite as well as the ideal distribution coefficients of the model reactions are listed in Table 1.

Table 1 Ideal activities of the mineral phases and distribution coefficients of the model reactions

Garnet
$X_{alm}^{Grt}=(X_{Fe}^{Grt})^3$, $X_{prp}^{Grt}=(X_{Mg}^{Grt})^3$, $X_{grs}^{Grt}=(X_{Ca}^{Grt})^3$, $X_{sps}^{Grt}=(X_{Mn}^{Grt})^3$,
$X_{Fe}^{Grt}=Fe^{2+}/(Fe^{2+}+Mg+Ca+Mn)$, $X_{Mg}^{Grt}=Mg/(Fe^{2+}+Mg+Ca+Mn)$,
$X_{Ca}^{Grt}=Ca/(Fe^{2+}+Mg+Ca+Mn)$, $X_{Mn}^{Grt}=Mn/(Fe^{2+}+Mg+Ca+Mn)$
Muscovite
$Al^{VI}=Al+Si-4$, $X_{Ms}^{Ms}=(X_{Al^{VI}}^{Ms})^2$, $X_{Mg\text{-}cel}^{Ms}=4(X_{Mg}^{Ms})(X_{Al^{VI}}^{Ms})$, $X_{Fe\text{-}cel}^{Ms}=4(X_{Fe}^{Ms})(X_{Al^{VI}}^{Ms})$,
$X_{Fe}^{Ms}=Fe^{2+}/(Fe^{2+}+Mg+Al^{VI})$, $X_{Mg}^{Ms}=Mg/(Fe^{2+}+Mg+Al^{VI})$, $X_{Al^{VI}}^{Ms}=Al^{VI}/(Fe^{2+}+Mg+Al^{VI})$
Distribution coefficients
$K_{D(1)}=\frac{(X_{alm}^{Grt})(X_{Mg\text{-}cel}^{Ms})^3}{(X_{prp}^{Grt})(X_{Fe\text{-}cel}^{Ms})^3}=\frac{(X_{Fe}^{Grt})^3(X_{Mg}^{Ms})^3}{(X_{Mg}^{Grt})^3(X_{Fe}^{Ms})^3}$, $K_{D(2)}=\frac{(X_{Fe\text{-}cel}^{Ms})^3}{(X_{alm}^{Grt})(X_{Ms}^{Ms})^3}=(\frac{4X_{Fe}^{Ms}}{X_{Fe}^{Grt}X_{Al^{VI}}^{Ms}})^3$, $K_{D(3)}=\frac{(X_{Mg\text{-}cel}^{Ms})^3}{(X_{prp}^{Grt})(X_{Ms}^{Ms})^3}=(\frac{4X_{Mg}^{Ms}}{X_{Mg}^{Grt}X_{Al^{VI}}^{Ms}})^3$

2.2 Activity Model of Garnet

In metapelitic garnet, the divalent cations Fe^{2+}, Mg^{2+}, Ca^{2+} and Mn^{2+} mix in the three equivalent hexahedral sites and the trivalent cations Fe^{3+}, Cr^{3+} and Al^{3+} occupy the two equivalent octahedral sites. In fact, the Fe^{3+} and Cr^{3+} cations are negligible due to extreme dilution, therefore, only the mixing properties of the divalent cations on the hexahedral sites are to be considered. Holdaway (2001) adopted averaged Margules parameters of the garnet activity models (Mukhopadhyay et al., 1997; Berman and Aranovich, 1996; Ganguly et al., 1996) in calibrating the GASP geobarometer. This non-ideal, asymmetric Fe-Mg-Ca-Mn quaternary activity model (Holdaway, 2001) was also used in calibrating the GMAQ geothermobarometers in this study. The excess chemical potential of the almandine and pyrope components in garnet (Holdaway, 2001), after rearrangement, may be written respectively as

$$RT\ln\gamma_{Alm}^{Grt}=3RT\ln(\gamma_{Fe}^{Grt})=Fea\cdot T(K)+Feb\cdot P(bar)+Fec \quad (7)$$

$$RT\ln\gamma_{Prp}^{Grt}=3RT\ln(\gamma_{Mg}^{Grt})=Mga\cdot T(K)+Mgb\cdot P(bar)+Mgc \quad (8)$$

in which Fea, Feb, Fec, Mga, Mgb and Mgc are polynomial expressions consisting of molar fractions of the Fe^{2+}, Mg^{2+}, Ca^{2+} and Mn^{2+} cations of garnet and are described in Table S2.

2.3 Activity Model of Muscovite

It should be stated that the activity model of tschermak in muscovite defined by Hodges and Crowley (1985) in their Table 4 is miswritten, such that this unique previous GMAQ barometer is hard to apply. Although the Fe^{2+} and Mg^{2+} cations in the two equivalent octahedral sites of muscovite are dilute, it has been found that the muscovite solid solution is not ideal. Therefore, muscovite may be considered as a non-ideal, symmetric Fe-Mg-Al^{VI} ternary solid solution. Adopting the symmetric formulations of ternary solid solutions of Mukhopadhyay et al. (1993), the excess chemical potential of Fe- and Mg-celadonite can be described respectively as

$$RT\ln\gamma_{Fe\text{-}Cel}^{Ms}=X_{Mg}^{Ms}(1-X_{Fe}^{Ms})W_{FeMg}^{Ms}+X_{Al}^{Ms}(1-X_{Fe}^{Ms})W_{FeAl}^{Ms}-X_{Mg}^{Ms}X_{Al}^{Ms}W_{MgAl}^{Ms} \quad (9)$$

$$RT\ln\gamma_{Mg\text{-}Cel}^{Ms}=X_{Fe}^{Ms}(1-X_{Mg}^{Ms})W_{FeMg}^{Ms}+X_{Al}^{Ms}(1-X_{Mg}^{Ms})W_{MgAl}^{Ms}-X_{Fe}^{Ms}X_{Al}^{Ms}W_{FeAl}^{Ms} \quad (10)$$

in which the W items are Margules parameters to be determined through statistical regression. Although complex activity models of muscovite have been proposed (e.g., Keller et al., 2005; Parra et al., 2003; Massonne and Szpurka, 1997), it is found that this symmetric ternary solution is sufficient to accurately calibrate the GMAQ thermobarometers.

2.4 Regression Models

Inserting the above activity models of garnet (Eqs. 7–8) and muscovite (Eqs. 9 and 10) into the equilibrium thermodynamic equations (Eqs. 4–6), the thermodynamic equilibria of the model reactions (Eqs. 1–3) may be described respectively by the following regression models

$$\begin{aligned}T=&(\Delta_1H^0/\Delta_1S^0)+[P(bar)-1]\cdot(\Delta_1V^0/\Delta_1S^0)+\\&(W_{FeMg}^{Ms}/\Delta_1S^0)\cdot3(X_{Fe}^{Ms}-X_{Mg}^{Ms})+\\&[(W_{MgAl}^{Ms}-W_{FeAl}^{Ms})/\Delta_1S^0]\cdot3X_{Al}^{Ms}+\\&(1/\Delta_1S^0)\cdot[RT\ln K_{D(1)}+(Fea-Mga)\cdot T+\\&(Feb-Mgb)\cdot P+(Fec-Mgc)]\end{aligned} \quad (11)$$

$$\begin{aligned}P_{Fe}=&1-\Delta_2H^0/\Delta_2V^0+T(\Delta_2S^0/\Delta_2V^0)+\\&(W_{FeAl}^{Ms}/\Delta_2V^0)\cdot3(X_{Fe}^{Ms}-X_{Al}^{Ms})+\\&[(W_{MgAl}^{Ms}-W_{FeMg}^{Ms})/\Delta_2V^0]\cdot3X_{Mg}^{Ms}+\\&(1/\Delta_2V^0)\{Feb\cdot P+Fec+T[Fea-R\ln K_{D(2)}]\}\end{aligned} \quad (12)$$

$$\begin{aligned}P_{Mg}=&1-\Delta_3H^0/\Delta_3V^0+T(\Delta_3S^0/\Delta_3V^0)+\\&(W_{MgAl}^{Ms}/\Delta_3V^0)\cdot3(X_{Mg}^{Ms}-X_{Al}^{Ms})+\\&[(W_{FeAl}^{Ms}-W_{FeMg}^{Ms})/\Delta_3V^0]\cdot3X_{Fe}^{Ms}+\\&(1/\Delta_3V^0)\{Mgb\cdot P+Mgc+T[Mga-R\ln K_{D(3)}]\}\end{aligned} \quad (13)$$

2.5 Calibration Results

Regressions of Eqs. (11)–(13) have been done using the natural metapelitic data (Table S1) and the results are listed in Table 2. The regressions were weighted, that is to say, the calibration samples were used in nearly equal quantities considering the pressure and temperature intervals. Substituting the regressed parameters (Table 2) into Eqs. (11)–(13), seven formulations (Eqs. 14–20) of the GMAQ thermobarometers have been obtained as the following.

Formulation of the garnet-muscovite thermometer

$$T(\mathrm{K})[100.0+0.7(R\ln K_{D(1)}+\mathrm{Fea}-\mathrm{Mga})] = 33\,648.0+[2.0-0.7(\mathrm{Feb}-\mathrm{Mgb})]P(\mathrm{bar})-0.7\mathrm{Fec}+0.7\mathrm{Mgc}-142\,260.0(X_{\mathrm{Fe}}^{\mathrm{Ms}}-X_{\mathrm{Mg}}^{\mathrm{Ms}})+68\,610.0X_{\mathrm{Al}}^{\mathrm{Ms}} \quad (14)$$

Formulations of the GMAQ barometer

$$P_{\mathrm{Fe}}^{\mathrm{And}}(1-0.098\mathrm{Feb})(\mathrm{bar}) = -16\,770.0+23.447T(\mathrm{K})+2\,367.3(X_{\mathrm{Fe}}^{\mathrm{Ms}}-X_{\mathrm{Al}}^{\mathrm{Ms}})-41\,951.7X_{\mathrm{Mg}}^{\mathrm{Ms}}+0.098\{\mathrm{Fec}+T[\mathrm{Fea}-R\ln K_{D(2)}]\} \quad (15)$$

$$P_{\mathrm{Fe}}^{\mathrm{Sil}}(1-0.162\mathrm{Feb})(\mathrm{bar}) = 13\,476.8+20.928T(\mathrm{K})+35\,684.4(X_{\mathrm{Fe}}^{\mathrm{Ms}}-X_{\mathrm{Al}}^{\mathrm{Ms}})-19\,350.9X_{\mathrm{Mg}}^{\mathrm{Ms}}+0.162\{\mathrm{Fec}+T[\mathrm{Fea}-R\ln K_{D(2)}]\} \quad (16)$$

$$P_{\mathrm{Fe}}^{\mathrm{Ky}}(1+0.242\mathrm{Feb})(\mathrm{bar}) = -61\,802.0+22.491T(\mathrm{K})-61\,578.0(X_{\mathrm{Fe}}^{\mathrm{Ms}}-X_{\mathrm{Al}}^{\mathrm{Ms}})+69\,441.5X_{\mathrm{Mg}}^{\mathrm{Ms}}-0.242\{\mathrm{Fec}+T[\mathrm{Fea}-R\ln K_{D(2)}]\} \quad (17)$$

$$P_{\mathrm{Mg}}^{\mathrm{And}}(1-0.021\mathrm{Mgb})(\mathrm{bar}) = -37\,962.6+24.991T(\mathrm{K})-22\,654.5(X_{\mathrm{Mg}}^{\mathrm{Ms}}-X_{\mathrm{Al}}^{\mathrm{Ms}})-19\,770.9X_{\mathrm{Fe}}^{\mathrm{Ms}}+0.021\{\mathrm{Mgc}+T[\mathrm{Mga}-R\ln K_{D(3)}]\} \quad (18)$$

$$P_{\mathrm{Mg}}^{\mathrm{Sil}}(1+0.089\mathrm{Mgb})(\mathrm{bar}) = -28\,742.5+22.705T(\mathrm{K})-15\,439.8(X_{\mathrm{Mg}}^{\mathrm{Ms}}-X_{\mathrm{Al}}^{\mathrm{Ms}})+3\,161.1X_{\mathrm{Fe}}^{\mathrm{Ms}}-0.089\{\mathrm{Mgc}+T[\mathrm{Mga}-R\ln K_{D(3)}]\} \quad (19)$$

$$P_{\mathrm{Mg}}^{\mathrm{Ky}}(1+0.035\mathrm{Mgb})(\mathrm{bar}) = -771.4+20.838T(\mathrm{K})+10\,840.2(X_{\mathrm{Mg}}^{\mathrm{Ms}}-X_{\mathrm{Al}}^{\mathrm{Ms}})-21\,704.5X_{\mathrm{Fe}}^{\mathrm{Ms}}-0.035\{\mathrm{Mgc}+T[\mathrm{Mga}-R\ln K_{D(3)}]\} \quad (20)$$

3 ERROR CONSIDERATION

It is found that 88% of the calibrant samples (Table S1) yield garnet-muscovite temperature consistent to the garnet-biotite temperature (Holdaway, 2000) within error of ±50 °C (Fig. 1a). Distribution of the difference between the garnet-muscovite and the garnet-biotite (Holdaway 2000) temperatures is almost unrelated to either temperature (Fig. 1b), or pressure (Fig. 1c), or composition of muscovite (Fig. 1d) or garnet (Fig. 1e), suggesting that this garnet-muscovite thermometer yields no bias estimates of temperature.

Meanwhile, it is found that 78% and 70% of the calibrant samples yield GMAQ-Fe and GMAQ-Mg pressures consistent to that of the GASP barometer (Holdaway, 2001) within error of ±1 kbar, respectively (Figs. 2a–2b). The GMAQ-Fe and GMAQ-Mg barometers yield identical pressure estimates within error of ±1 kbar for 95% of the calibrant samples (Fig. 2c), suggesting that both the Fe- and Mg-endmember model reactions are equivalent. The garnet-biotite thermometer (Holdaway, 2000) combined with the GASP barometer (Holdaway, 2001) plot the calibrant samples into the correct stability field of the Al_2SiO_5 polymorphs (Fig. 2d), as do the GMAQ-Fe (Fig. 2e) and GMAQ-Mg (Fig. 2f) barometers based on the garnet-biotite thermometer (Holdaway, 2000). When simultaneously applying the garnet-muscovite thermometer and the GMAQ-Fe and GMAQ-Mg barometers, most of the samples have also been plotted into the correct stability field of the

Table 2 Regression summary in calibrating the garnet-muscovite thermometer and the GMAQ barometer

(a) The garnet-muscovite (GM) geothermometer

Δ_1H^0/Δ_1S^0 (K)	Δ_1V^0/Δ_1S^0 (K/bar)	$W_{\mathrm{FeMg}}^{\mathrm{Ms}}/\Delta_1S^0$ (K)	$(W_{\mathrm{MgAl}}^{\mathrm{Ms}}-W_{\mathrm{FeAl}}^{\mathrm{Ms}})/\Delta_1S^0$ (K)	$1/\Delta_1S^0$ (K/J)	R
336.5 (±66.9)	0.020 (±0.001)	-474.2 (±63.0)	228.7 (±26.7)	-0.007 (±0.001)	0.858

(b) The garnet-muscovite-Al_2SiO_5-quartz (GMAQ) geobarometer

	Δ_2H^0/Δ_2V^0 (bar)	Δ_2S^0/Δ_2V^0 (bar/K)	$W_{\mathrm{FeAl}}^{\mathrm{Ms}}/\Delta_2V^0$ (bar)	$(W_{\mathrm{MgAl}}^{\mathrm{Ms}}-W_{\mathrm{FeMg}}^{\mathrm{Ms}})/\Delta_2V^0$ (bar)	$1/\Delta_2V^0$ (bar/J)	R
P_{Fe} (And)	16 771.0 (±10 179.9)	23.447 (±7.975)	789.1 (±3 656.5)	-13 983.9 (±10 542.0)	0.098 (±0.044)	0.957
P_{Fe} (Sil)	-13 475.8 (±5 949.0)	20.928 (±1.278)	11 894.8 (±2 515.3)	-6 450.3 (±2 020.3)	0.162 (±0.032)	0.830
P_{Fe} (Ky)	61 803.0 (±6 920.3)	22.491 (±1.222)	-20 526.0 (±2 708.1)	23 147.2 (±2 165.9)	-0.242 (±0.033)	0.912
	Δ_3H^0/Δ_3V^0 (bar)	Δ_3S^0/Δ_3V^0 (bar/K)	$W_{\mathrm{MgAl}}^{\mathrm{Ms}}/\Delta_3V^0$ (bar)	$(W_{\mathrm{FeAl}}^{\mathrm{Ms}}-W_{\mathrm{FeMg}}^{\mathrm{Ms}})/\Delta_3V^0$ (bar)	$1/\Delta_3V^0$ (bar/J)	R
P_{Mg} (And)	37 963.6 (±20 080.9)	24.991 (±8.843)	-7 551.5 (±6 367.2)	-6 590.3 (±6 654.6)	0.021 (±0.048)	0.946
P_{Mg} (Sil)	28 743.5 (±3 529.9)	22.705 (±1.274)	-5 146.6 (±1 072.8)	1 053.7 (±1 204.4)	-0.089 (±0.014)	0.842
P_{Mg} (Ky)	772.4 (±4 309.0)	20.838 (±1.539)	3 613.4 (±1 272.5)	-7 234.8 (±2 241.6)	-0.035 (±0.019)	0.881

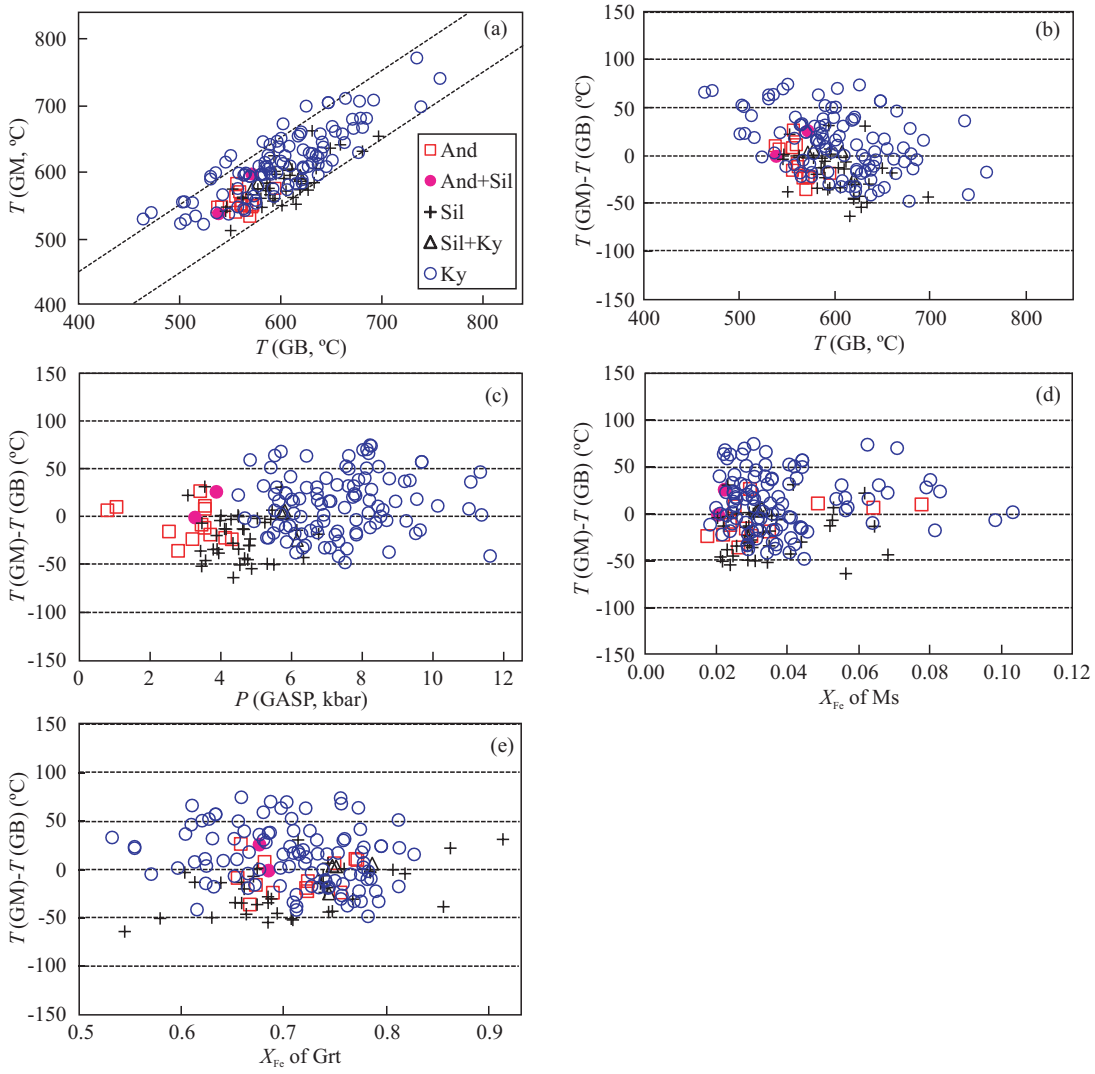

Figure 1. Temperature estimated by the garnet-muscovite vs. the garnet-biotite (Holdaway, 2000) geothermometers (a), and the relationships of the random error of the garnet-muscovite geothermometer with temperature (b), pressure (c), composition of muscovite (d) and composition of garnet (e), respectively. *T* (GM) and *T* (GB) are temperatures determined by the present garnet-muscovite and the garnet-biotite (Holdaway, 2000) geothermometers, respectively. It is seen that the random error of the present garnet-muscovite thermometer shows no bias with *P*, *T* and compositions of both garnet and muscovite. Dashed lines represent ±50 °C deviation.

Al_2SiO_5 polymorphs (Figs. 2g–2h). Furthermore, distribution of the difference between the GMAQ and GASP (Holdaway, 2001) pressures is independent of either pressure (Figs. 3a–3b) or temperature (Figs. 3c–3d) or chemical composition of muscovite (Figs. 3e–3f) or garnet (Figs. 3g–3h).

The precision of the garnet-muscovite thermometer and the GMAQ barometer cannot be determined at present due to lack of phase equilibrium experimental data. However, the random errors of these thermobarometers can be roughly estimated. It should be noted that due to complex formulations of these thermobarometers, standard error propagation estimation (cf. Kohn and Spear, 1991) cannot be done. Under such circumstances, we can only estimate their random errors by semi-quantitative methods, based on the calibration data listed in Table S1.

3.1 Random Errors of the Garnet-Muscovite Thermometer

The random errors of the garnet-muscovite thermometer mainly come from the errors of input pressures as well as chemical compositions of garnet and muscovite. Errors of ±1 kbar of input *P* translate to *T* errors of ±10–17 °C. Analytical errors of ±2% of Fe and Mg of muscovite translate to *T* errors of ±1–2 and ±1–3 °C, respectively. As those for garnet, the translated *T* errors are of ±2–4 and ±2–4 °C, respectively. The errors of analytical sources are almost unrelated. When combining the various errors as described above, it may be concluded that the total random error of the garnet-muscovite thermometer is around ca. ±60 °C.

3.2 Random Errors of the GMAQ Barometer

The random errors of the GMAQ barometers mainly come from the errors of input temperatures and also from analytical errors of chemical compositions of garnet and muscovite. As for the Fe-endmember GMAQ barometer, an input *T* error of ±50 °C may translate to GMAQ *P* errors of ±0.3–1.4 kbar. The analytical errors of ±2% of Fe in muscovite and garnet, may

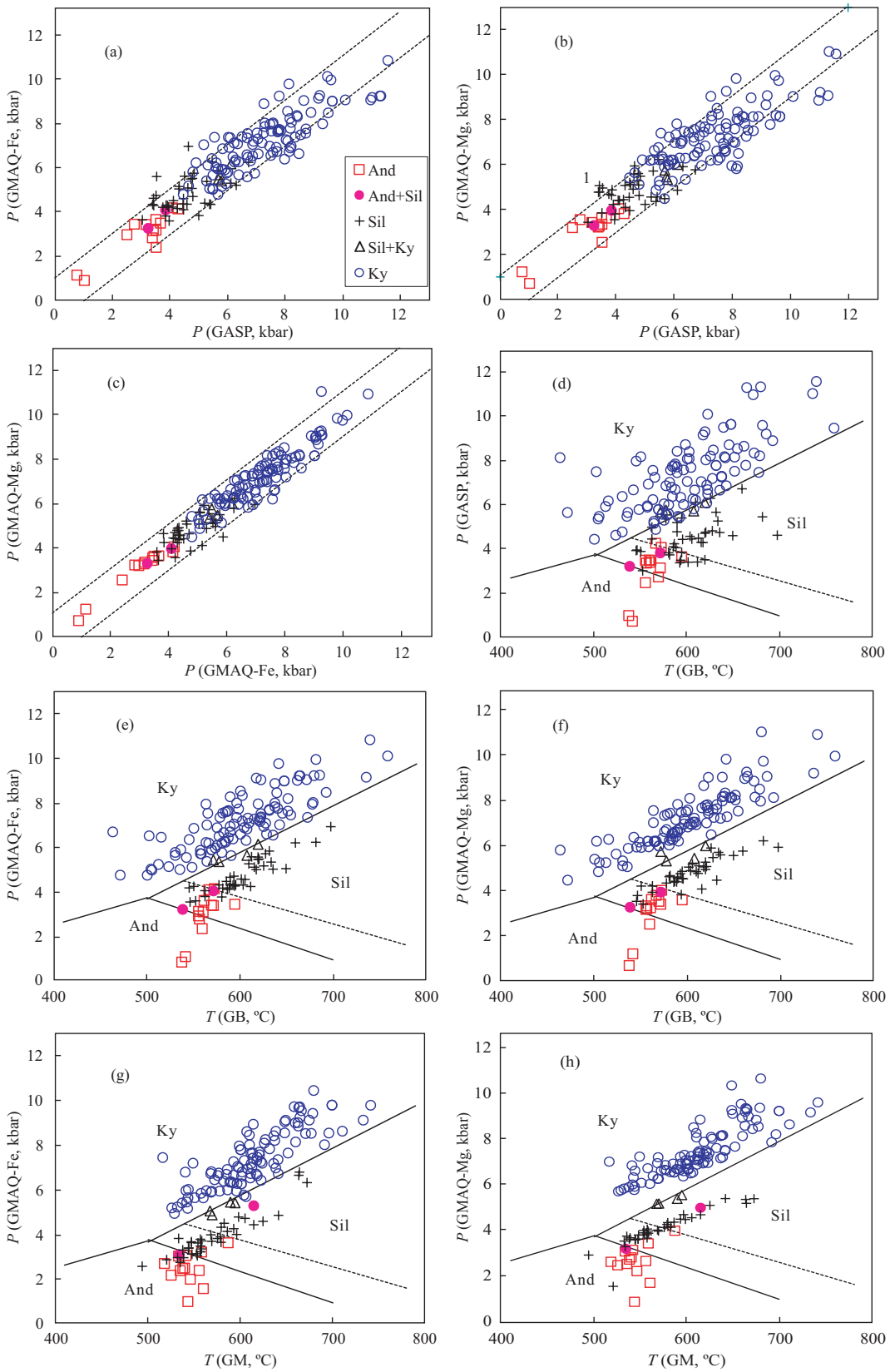

Figure 2. (a), (b) Pressure computed by the GASP geobarometer (Holdaway, 2001) vs. the present GMAQ geobarometer. (c) The Fe- and Mg-endmember GMAQ barometer yields identical pressure estimates within error of ±1 kbar. (d) The metapelitic samples are plotted into the correct stability field of the Al_2SiO_5 polymorphs by both the GASP geobarometer. (e), (f) The GMAQ geobarometer in concert with the garnet-biotite temperature (Holdaway, 2000). (g), (h) When simultaneously applying the present garnet-muscovite thermometer and the GMAQ geobarometer, most of these metapelites are also accurately plotted into the correct stability field. Dashed lines in (a)–(c) represent ±1 kbar deviation. The Al_2SiO_5 polyphase diagrams (g)–(h) are from Holdaway and Mukhopadhay (1993) and the dashed line is from Pattison (1992).

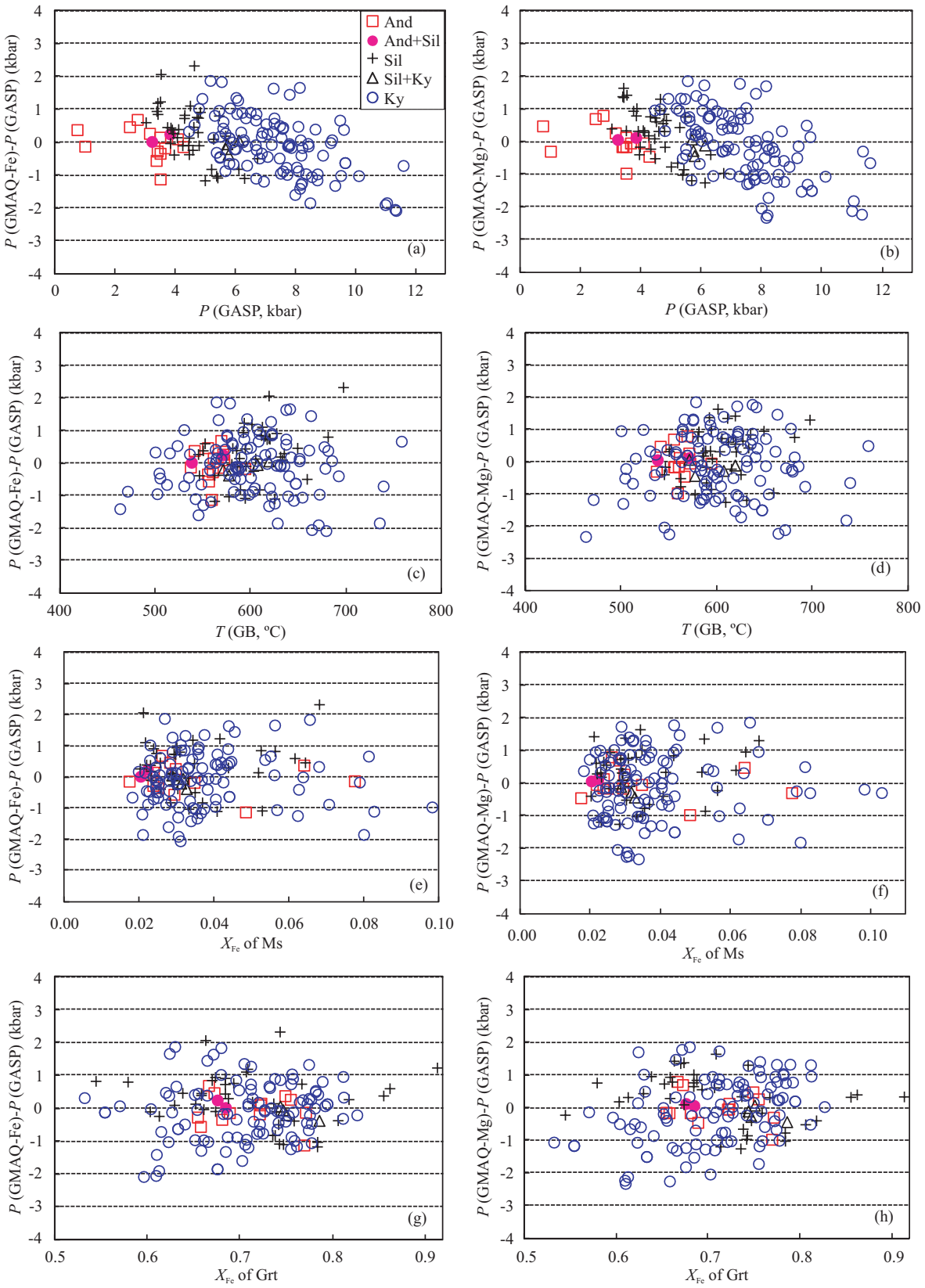

Figure 3. Random error of the GMAQ geobarometer vs. temperature (a), (b), pressure (c), (d), compositions of muscovite (e), (f) and garnet (g), (h), respectively, suggesting that the GMAQ geobarometer has no systematic bias.

translate to GMAQ *P* errors of ±0.07–0.12 and ±0.03–0.06 kbar, respectively. Thus, the total random error of the Fe-endmember GMAQ barometer is estimated to be of ca. ±1.5 kbar. Similarly, the total random error of the Mg-endmember GMAQ barometer is inferred to be of ca. ±1.4 kbar.

4 APPLICATIONS OF THE GMAQ THERMOBAROMETERS

The garnet-muscovite thermometer and GMAQ barometer calibrated in this work are applied to natural metamorphic terranes to test their applicability. When Al_2SiO_5 minerals are present the thermometer and the barometers are simultaneously applied by iteration. When no Al_2SiO_5 minerals are present, assumed pressures are input to obtain garnet-muscovite temperatures. Retrograded mineral assemblages were excluded in the following.

4.1 Application of the Garnet-Muscovite Thermometer

A valid thermometer should clearly discriminate the systematic temperature change of different zones within either a prograde or an inverted metamorphic terrane or a thermal contact aureole, as suggested by Wu and Chang (2006). Validity of the present thermometer was checked through its applications to world-wide metamorphic terranes hereafter. The results are given in Table S3.

The Barrovian type metamorphic sequences have been found in the Snow Peak area, northern Idaho, USA (Lang and Rice, 1985). The metamorphic grade progressively increases from the chlorite-biotite, garnet, staurolite, transition, staurolite-kyanite and the kyanite zones in sequence. These zones were metamorphosed in a second metamorphic event M2 and the mineral assemblages are post-kinematic. Both the garnet-biotite thermometer (Holdaway, 2000) and the garnet-muscovite thermometer clearly reflect the expected systematic temperature change (Table S3; Fig. 4a).

A complete Barrovian metamorphic sequence ranges gradually from the chlorite, biotite, garnet, lower staurolite, upper staurolite, kyanite, sillimanite to the sillimanite-K-feldspar zones in the metapelitic gneisses in a region extending from the Hudson River in south-eastern New York State, to the high-grade core of the Taconic range in western Connecticut, USA (Whitney et al., 1996). In the chlorite and biotite zones garnet is absent and thus the temperatures cannot be determined. The garnet of the garnet zone is MnO-rich which exceeds the X_{Mn} limit for both the garnet-biotite and garnet-muscovite thermometers, and thus the garnet activity model is invalid for MnO-rich garnet, therefore, unexpected high temperatures were obtained. For the lower staurolite, upper staurolite, kyanite, sillimanite to the sillimanite-K-feldspar zones, both the garnet-biotite (Holdaway, 2000) and the garnet-muscovite temperatures sequentially increase (Table S3; Fig. 4b).

The Lower Paleozoic Silgará Formation in the southwestern Santander massif was affected by Caledonian regional metamorphism, which created a Barrovian-type sequence of metamorphic zones (biotite, garnet, staurolite and sillimanite) increasing from the SE to the NW (Ríos et al., 2003). The garnet-biotite (Holdaway, 2000) and the garnet-muscovite thermometers confirmed the gradual temperature increase (Table S3; Fig. 4c).

The Danba domal metamorphic terrane, eastern edge of the Qinghai-Xizang Plateau, western China, is characterized by prograde Barrovian type metamorphic sequence during the late Indosinian crustal thickening and shortening (Huang et al., 2003). From the low grade biotite zone to the concentric garnet, staurolite, kyanite and sillimanite zones, both the garnet-biotite (Holdaway, 2000) and the garnet-muscovite temperatures gradually increase (Table S3; Fig. 4d). It is noted that the garnet-

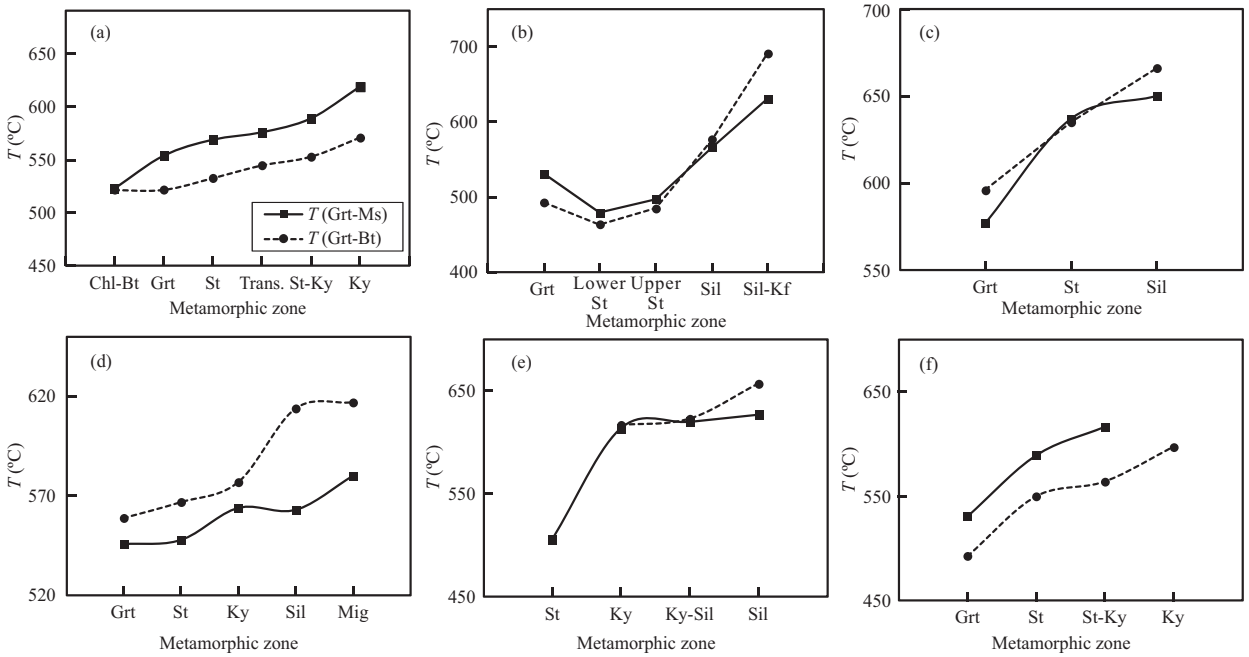

Figure 4. Application of the present garnet-muscovite geothermometer to the prograde metamorphic terranes suggests that the thermometer successfully reflects the gradual temperature change of the different metamorphic zones. (a) The Snow Peak Barrovian type metamorphic sequences, northern Idaho, USA (Lang and Rice, 1985); (b) the Barrovian metamorphic zones of the Dutchess County, New York, USA (Whitney et al., 1996); (c) the prograde metamorphic terrane of the Silgará Formation, southwestern Santander massif, Colombian Andes (Ríos et al., 2003); (d) the Danba Barrovian-type metamorphic terrane, Sichuan, China (Huang et al., 2003); (e) the Danba Barrovian-type metamorphic terrane, Sichuan, China (Weller et al., 2013); and (f) the prograde metamorphic zones of the central Menderes massif, Turkey (Ashworth and Evirgen, 1985a, b).

biotite temperature of the highest migmatite zone is lower than the next highest sillimanite zone, possibly due to post-peak Fe-Mg re-exchange between garnet and biotite. Again, the garnet-biotite (Holdaway, 2000) and the garnet-muscovite thermometers reflect such a *T*-increasing trend for another sampling traverse (Weller et al., 2013) including the staurolite, kyanite, kyanite-sillimanite and the sillimanite zones (Table S3; Fig. 4e).

An orderly prograde metamorphic zonation appears sequentially, including garnet, staurolite, staurolite-kyanite and kyanite zones in the central Menderes massif, Turkey (Ashworth and Evirgen, 1985a, b). Again, both the garnet-biotite (Holdaway, 2000) and the garnet-muscovite thermometers clearly discriminated the systematic temperature change of these zones (Table S3; Fig. 4f).

The High Himalaya crystalline zone and the main central thrust as well as the Lesser Himalaya have long been recognized as inverted metamorphic zones. In the 6-km-long exposure near the Village Atholi, Chenab River Gorge, Kashmir, the main central thrust appears as an inverted metamorphic belt (Stephenson et al., 2000). From the bottom to the top, there sequentially exposes the garnet, staurolite and the kyanite zones. Both the garnet-biotite (Holdaway, 2000) and the garnet-muscovite thermometers record the inverted temperature change of these zones (Table S3; Fig. 5a). Also in the Sutlej Valley, Himachal Pradesh, the High Himalaya crystalline zone, there exposes an inverted metamorphic sequence (Vannay and Grasemann, 1998). The garnet-biotite (Holdaway, 2000) and the garnet-muscovite thermometers confirm such an inversion of metamorphic temperatures of the sillimanite, kyanite and staurolite zones (Table S3; Fig. 5b). As for the migmatite zone, both the garnet-biotite (Holdaway, 2000) and the garnet-muscovite thermometers yielded lower temperature than that of the sillimanite zone, possibly due to post-peak Fe-Mg re-exchange between garnet and muscovite (Fig. 5b). Or alternatively, muscovite might be formed at the retrogressive stage.

Holdaway et al. (1988) found that five regional contact metamorphic events (M1–M5) occurred in the Devonian and Carboniferous in west-central Maine, USA, among which the M3 and M5 events are the two most important metamorphic events. Each metamorphic event is closely associated with emplacement of S-type granites, such that the isograd patterns produced in the surrounding pelitic schists generally mirror the geometry of plutonic intrusive contacts. From north to south the metamorphic grade varies from the chlorite to garnet, staurolite, sillimanite and the K-feldspar-sillimanite zones, and from low to high grades these zones are designated as Grades 3, 4, 5, 6 (M3) and Grades 6.5, 7 and 8 (M5), respectively (Holdaway et al., 1988). Both the garnet-biotite (Holdaway, 2000) and the garnet-muscovite thermometers demonstrate such a *T*-increasing trend (Table S3; Fig. 6a).

The present garnet-muscovite geothermometer was also applied to the contact metamorphosed Fe- and Al-rich graphitic metapelite, the Transangarian region of the Yenisei Ridge, eastern Siberia, Russia (Likhanov et al., 2001). It has been shown that from the garnet, andalusite, lower to the upper cordierite zones, the garnet-biotite (Holdaway, 2000) and the garnet-muscovite temperatures gradually increase (Table S3; Fig. 6b), except for one garnet zone sample which temperature was over-estimated

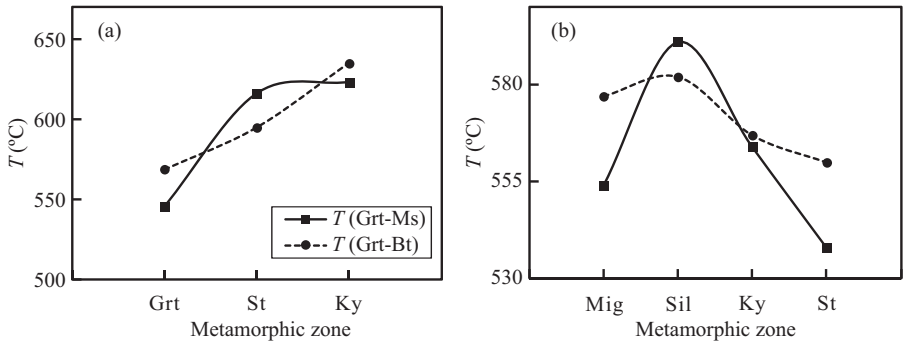

Figure 5. Application of the garnet-muscovite geothermometer to (a) the inverted metamorphic zone of the Main Central Thrust, the Kishtwar Window, Himalaya (Stephenson et al., 2000); and (b) the inverted metamorphic terrane, the High Himalaya crystalline zone, Himachal Pradesh (Vannay and Grasemann, 1998).

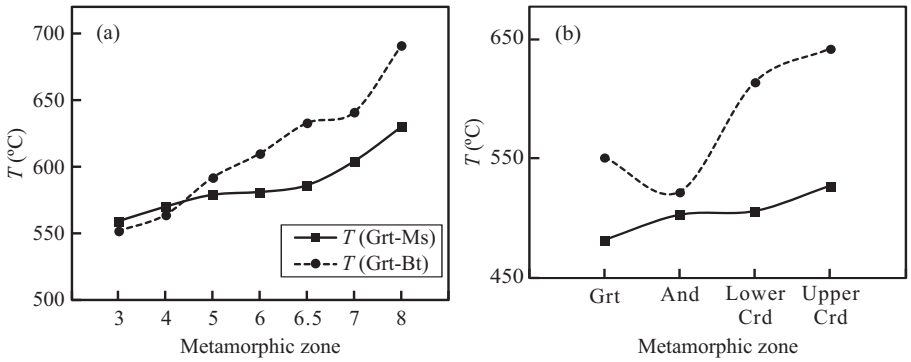

Figure 6. Application of the garnet-muscovite geothermometer to (a) the regional thermal contact aureoles, west-central Maine, USA (Holdaway et al., 1988); and (b) the thermal contact aureole, Transangarian, the Yenisei Ridge, Russia (Likhanov et al., 2001).

by the garnet-biotite geothermometer (Holdaway, 2000).

It is found that the present garnet-muscovite thermometer is slightly more accurate than the previous versions (Wu and Zhao, 2006a; Wu et al., 2002; Hynes and Forest, 1988; Green and Hellman, 1982; Krogh and Råheim, 1978). For clarity, the comparison is not listed.

4.2 Application of the GMAQ Barometer

As outlined in Wu and Cheng (2006) in evaluating the accuracy of the GASP barometer, a valid GMAQ barometer should also meet the following criteria: (1) samples should be plotted into the correct Al_2SiO_5 polymorph stability field, and the transition boundaries of the Al_2SiO_5 polymorphs should be correctly discerned; (2) in general, rocks within a very limited geographic area without post-metamorphic structural discontinuity, should show no obvious pressure diversity; and (3) rocks formed at thermodynamic equilibrium within a limited contact aureole should record constant GMAQ pressure.

For the regional thermal contact aureoles, west-central Maine, USA (Holdaway et al., 1988), except for few samples, the metamorphic pressures were determined to be of 3.3–4.3 and 3.7–4.4 kbar by simultaneously applying the garnet-muscovite thermometer and the Fe- and Mg-endmember GMAQ barometers (Table S3). The averaged GMAQ pressures are 3.8 and 4.1 kbar for the two GMAQ barometers, respectively, about 1 kbar lower than that of the GASP barometer (Holdaway, 2001), within error.

In the Augusta quadrangle thermal contact aureole, south-central Maine, USA (Novak and Holdaway, 1981), plagioclase does not exist in the metapelite, thus the GASP barometer (Holdaway, 2001) cannot be applied to determine the metamorphic pressure. Here, metamorphic pressures were estimated to be between 2.3–3.9 and 2.8–4.2 kbar by simultaneously applying the garnet-muscovite thermometer and the Fe- and Mg-endmember GMAQ barometers (Table S3) and the averaged pressures are 3.1 and 3.2 kbar, respectively, consistent to the ubiquitous presence of andalusite.

Finally, the garnet-muscovite thermometer and the GMAQ barometer were applied to the kyanite-bearing metapelite exposing along a 500 m-long traverse in a road side near the Hunt Valley Mall, northern Baltimore, Maryland, USA (Lang, 1991). The pressures are estimated to be in the range of 6.2–7.1 and 6.8–7.4 kbar, respectively, retrieved from the Fe- and Mg-endmember GMAQ barometers (Table S3), and the averaged values of 6.7 and 7.1 kbar are similar to that of 5.6 kbar derived from the GASP barometer (Holdaway, 2001), within error.

5 CONCLUSIONS

(1) The garnet-muscovite thermometer yields similar temperature estimates with the well-calibrated garnet-biotite thermometer for the crustal metapelite within errors of ±50 °C, and successfully discriminates the systematic temperature change of different zones of either prograde or inverted metamorphic terranes or thermal contact aureoles. The total random error of this thermometer is inferred to be around ±60 °C.

(2) Simultaneously applying the garnet-muscovite thermometer and the GMAQ barometer have plotted most of the Al_2SiO_5-bearing metapelitic samples into the correct stability field of Al_2SiO_5 polymorphs.

(3) The GMAQ barometer yields similar pressure values to the well-calibrated garnet-Al_2SiO_5-plagioclase-quartz (GASP) barometer within errors of ±1 kbar. When the GMAQ barometer is applied to metapelite within limited geographic area or thermal contact aureole, the respective constant pressure is obtained. The total random error of the GMAQ barometer is inferred to be of ca. ±1.4 kbar.

A spreadsheet (Table S4) in simultaneously applying the garnet-muscovite thermometer and the GMAQ barometer can be found in the journal's website as an electronic appendix.

ACKNOWLEDGMENTS

The quality of this paper has been improved through reviews by two referees. This research was supported by the Key Research Program of Frontier Sciences of Chinese Academy of Sciences (No. QYZDJ-SSW-DQC036) and the National Natural Science Foundation of China (No. 41730215). This paper is in honour of Prof. Zhendong You (China University of Geosciences, Wuhan) dedicated to his contributions to metamorphic geology on his 90th birthday. The final publication is available at Springer via https://doi.org/10.1007/s12583-018-0851-z.

Electronic Supplementary Materials: Supplementary materials (Tables S1–S4) are available in the online version of this article at https://doi.org/10.1007/s12583-018-0851-z.

REFERENCES CITED

Ali, A., Yar, M., Khan, M. A., et al., 2016. Interrelationships between Deformation and Metamorphic Events across the Western Hinterland Zone, NW Pakistan. *Journal of Earth Science*, 27(4): 584–598. https://doi.org/10.1007/s12583-016-0717-1

Ashworth, J. R., Evirgen, M. M., 1985a. Plagioclase Relations in Pelites, Central Menderes Massif, Turkey. I. the Peristerite Gap with Coexisting Kyanite. *Journal of Metamorphic Geology*, 3(3): 207–218. https://doi.org/10.1111/j.1525-1314.1985.tb00317.x

Ashworth, J. R., Evirgen, M. M., 1985b. Plagioclase Relations in Pelites, Central Menderes Massif, Turkey. II. Perturbation of Garnet-Plagioclase Geobarometers. *Journal of Metamorphic Geology*, 3(3): 219–229. https://doi.org/10.1111/j.1525-1314.1985.tb00318.x

Bell, T. H., Johnson, S. E., Davis, B., et al., 1992. Porphyroblast Inclusion-Trail Orientation Data: Eppure Non Son Girate!. *Journal of Metamorphic Geology*, 10(3): 295–307. https://doi.org/10.1111/j.1525-1314.1992.tb00084.x

Bell, T. H., Mares, V. M., 1999. Correlating Deformation and Metamorphism around Orogenic Arcs. *American Mineralogist*, 84(11/12): 1727–1740. https://doi.org/10.2138/am-1999-11-1203

Berman, R. G., 1991. Thermobarometry Using Multi-Equilibrium Calculations: A New Technique, with Petrological Applications. *Canadian Mineralogist*, 29: 833−855

Berman, R. G., Aranovich, L. Y., 1996. Optimized Standard State and Solution Properties of Minerals. I. Calibration for Olivine, Orthopyroxene, Cordierite, Garnet, and Ilmenite in the System FeO-MgO-CaO-Al_2O_3-TiO_2-SiO_2. *Contributions to Mineralogy and Petrology*, 126: 1–24

Bohlen, S. R., Liotta, J. J., 1986. A Barometer for Garnet Amphibolites and Garnet Granulites. *Journal of Petrology*, 27(5): 1025–1034. https://doi.org/10.1093/petrology/27.5.1025

Bohlen, S. R., Wall, V. J., Boettcher, A. L., 1983. Experimental Investigations and Geological Applications of Equilibria in the System FeO-TiO_2-Al_2O_3-SiO_2-H_2O. *American Mineralogist*, 68: 1049–1058

Chatterjee, N., 2016. Constraints from Monazite and Xenotime Growth Modelling in the MnCKFMASH-PYCe System on the *P-T* Path of a Metapelite from Shillong-Meghalaya Plateau: Implications for the Indian Shield Assembly. *Journal of Metamorphic Geology*, 35(4): 393–412. https://doi.org/10.1111/jmg.12237

Chen, N.-S., 1990. The *P-T* Paths of Qinling Group and Their Implications for the Evolution of Metamorphic Environment, Tectonism and Magmatism. *Earth Science—Journal of China University of Geosciences*, 15: 145–155 (in Chinese with English Abstract)

Chen, N.-S., Gong, S. L., Sun, M., et al., 2009. Precambrian Evolution of the Quanji Block, Northeastern Margin of Tibet: Insights from Zircon U-Pb and Lu-Hf Isotope Compositions. *Journal of Asian Earth Sciences*, 35(3/4): 367–376. https://doi.org/10.1016/j.jseaes.2008.10.004

Chen, N.-S., Sun, M., You, Z. D., et al., 1998. Well-Preserved Garnet Growth Zoning in Granulite from the Dabie Mountains, Central China. *Journal of Metamorphic Geology*, 16(2): 213–222. https://doi.org/10.1111/j.1525-1314.1998.00074.x

Cheng, S. H., Lai, X. Y., You, Z. D., 2009. *P-T* Paths Derived from Garnet Growth Zoning in Danba Domal Metamorphic Terrain, Sichuan Province, West China. *Journal of Earth Science*, 20(2): 219–240. https://doi.org/10.1007/s12583-009-0022-3

Ferry, J. M., Spear, F. S., 1978. Experimental Calibration of the Partitioning of Fe and Mg between Biotite and Garnet. *Contributions to Mineralogy and Petrology*, 66(2): 113–117. https://doi.org/10.1007/bf00372150

Ferry, J. M., Watson, E. B., 2007. New Thermodynamic Models and Revised Calibrations for the Ti-in-Zircon and Zr-in-Rutile Thermometers. *Contributions to Mineralogy and Petrology*, 154(4): 429–437. https://doi.org/10.1007/s00410-007-0201-0

Ganguly, J., Cheng, W. J., Tirone, M., 1996. Thermodynamics of Aluminosilicate Garnet Solid Solution: New Experimental Data, an Optimized Model, and Thermometric Applications. *Contributions to Mineralogy and Petrology*, 126(1/2): 137–151. https://doi.org/10.1007/s004100050240

Green, T. H., Hellman, P. L., 1982. Fe-Mg Partitioning between Coexisting Garnet and Phengite at High Pressure, and Comments on a Garnet-Phengite Geothermometer. *Lithos*, 15(4): 253–266. https://doi.org/10.1016/0024-4937(82)90017-2

Hodges, K. V., Crowley, P. D., 1985. Error Estimation and Empirical Geothermobarometry for Pelitic Systems. *American Mineralogist*, 70(7/8): 702–709

Holdaway, M. J., 2000. Application of New Experimental and Garnet Margules Data to the Garnet-Biotite Geothermometer. *American Mineralogist*, 85(7/8): 881–892. https://doi.org/10.2138/am-2000-0701

Holdaway, M. J., 2001. Recalibration of the GASP Geobarometer in Light of Recent Garnet and Plagioclase Activity Models and Versions of the Garnet-Biotite Geothermometer. *American Mineralogist*, 86(10): 1117–1129. https://doi.org/10.2138/am-2001-1001

Holdaway, M. J., Dutrow, B. L., Hinton, R. W., 1988. Devonian and Carboniferous Metamorphism in West-Central Maine: The Muscovite-Almandine Geobarometer and the Staurolite Problem Revised. *American Mineralogist*, 73: 20−47

Holdaway, M. J., Mukhopadhyay, B., 1993. A Re-evaluation of the Stability Relations of Andalusite: Thermochemical Data and Phase Diagram for the Alumino Silicates. *American Mineralogist*, 78: 298–315

Huang, M. H., Buick, I. S., Hou, L. W., 2003. Tectonometamorphic Evolution of the Eastern Tibet Plateau: Evidence from the Central Songpan-Garze Orogenic Belt, Western China. *Journal of Petrology*, 44(2): 255–278. https://doi.org/10.1093/petrology/44.2.255

Hynes, A., Forest, R. C., 1988. Empirical Garnet-Muscovite Geothermometry in Low-Grade Metapelites, Selwyn Range (Canadian Rockies). *Journal of Metamorphic Geology*, 6(3): 297–309. https://doi.org/10.1111/j.1525-1314.1988.tb00422.x

Johnson, S. E., 1999. Porphyroblast Microstructures: A Review of Current and Future Trends. *American Mineralogist*, 84(11/12): 1711–1726. https://doi.org/10.2138/am-1999-11-1202

Jones, K. A., 1994. Progressive Metamorphism in a Crustal-Scale Shear Zone: An Example from the Léon Region, North-West Brittany, France. *Journal of Metamorphic Geology*, 12(1): 69–88. https://doi.org/10.1111/j.1525-1314.1994.tb00004.x

Keller, L. M., de Capitani, C., Abart, R., 2005. A Quaternary Solution Model for White Micas Based on Natural Coexisting Phengite-Paragonite Pairs. *Journal of Petrology*, 46(10): 2129–2144. https://doi.org/10.1093/petrology/egi050

Kleemann, U., Reinhardt, J., 1994. Garnet-Biotite Thermometry Revisited: The Effect of Al^{VI} and Ti in Biotite. *European Journal of Mineralogy*, 6(6): 925–942. https://doi.org/10.1127/ejm/6/6/0925

Kohn, M. J., Spear, F. S., 1991. Error Propagation for Barometers: 2. Application to Rocks. *American Mineralogist*, 76: 138−147

Koziol, A. M., Newton, R. C., 1988. Redetermination of the Anorthite-Breakdown Reaction and Improvement of the Plagioclase-Garnet-Al_2SiO_5-Quartz Geobarometer. *American Mineralogist*, 73: 216–233

Krogh, E. J., Råheim, A., 1978. Temperature and Pressure Dependence of Fe-Mg Partitioning between Garnet and Phengite, with Particular Reference to Eclogites. *Contributions to Mineralogy and Petrology*, 66(1): 75–80. https://doi.org/10.1007/bf00376087

Lang, H. M., 1991. Quantitative Interpretation of Within-Outcrop Variation in Metamorphic Assemblages in Staurolite-Kyanite-Grade Metapelite, Baltimore, Maryland. *Canadian Mineralogist*, 29: 655−671

Lang, H. M., Rice, J. M., 1985. Regression Modelling of Metamorphic Reactions in Metapelites, Snow Peak, Northern Idaho. *Journal of Petrology*, 26(4): 857–887. https://doi.org/10.1093/petrology/26.4.857

Li, S. Z., Zhao, G. C., Santosh, M., et al., 2011. Palaeoproterozoic Tectonothermal Evolution and Deep Crustal Processes in the Jiao-Liao-Ji Belt, North China Craton: A Review. *Geological Journal*, 46(6): 525–543. https://doi.org/10.1002/gj.1282

Li, S. Z., Zhao, G. C., Sun, M., et al., 2005. Deformation History of the Paleoproterozoic Liaohe Assemblage in the Eastern Block of the North China Craton. *Journal of Asian Earth Sciences*, 24(5): 659–674. https://doi.org/10.1016/j.jseaes.2003.11.008

Li, S. Z., Zhao, G. C., Wilde, S. A., et al., 2010. Deformation History of the Hengshan-Wutai-Fuping Complexes: Implications for the Evolution of the Trans-North China Orogen. *Gondwana Research*, 18(4): 611–631. https://doi.org/10.1016/j.gr.2010.03.003

Likhanov, I. I., Reverdatto, V. V., Sheplev, V. S., et al., 2001. Contact Metamorphism of Fe- and Al-Rich Graphitic Metapelites in the Transangarian Region of the Yenisei Ridge, Eastern Siberia, Russia. *Lithos*, 58(1/2): 55–80. https://doi.org/10.1016/s0024-4937(01)00048-2

Maldonado, R., Weber, B., Ortega-Gutiérrez, F., et al., 2018. High-Pressure Metamorphic Evolution of Eclogite and Associated Metapelite from the Chuacús Complex (Guatemala Suture Zone): Constraints from Phase Equilibria Modelling Coupled with Lu-Hf and U-Pb Geochronology. *Journal of Metamorphic Geology*, 36(1): 95–124. https://doi.org/10.1111/jmg.12285

Massonne, H.-J., Szpurka, Z., 1997. Thermodynamic Properties of White Micas on the Basis of High-Pressure Experiments in the Systems K_2O-MgO-$A1_2O_3$-SiO_2-H_2O and K_2O-FeO-$A1_2O_3$-SiO_2-H_2O. *Lithos*, 41(1/2/3): 229–250. https://doi.org/10.1016/s0024-4937(97)82014-2

Mukhopadhyay, B., Basu, S., Holdaway, M. J., 1993. A Discussion of

Margules-Type Formulations for Multicomponent Solutions with a Generalized Approach. *Geochimica et Cosmochimica Acta*, 57(2): 277–283. https://doi.org/10.1016/0016-7037(93)90430-5

Mukhopadhyay, B., Holdaway, M. J., Koziol, A. M., 1997. A Statistical Model of Thermodynamic Mixing Properties of Ca-Mg-Fe^{2+} Garnets. *American Mineralogist*, 82(1/2): 165–181. https://doi.org/10.2138/am-1997-1-219

Novak, J. M., Holdaway, M. J., 1981. Metamorphic Petrology, Mineral Equilibria, and Polymetamorphism in the Augusta Quadrangle, South-Central Maine. *American Mineralogist*, 66: 51−69

Parra, T., Vidal, O., Agard, P., 2003. A Thermodynamic Model for Fe-Mg Dioctahedral K White Micas Using Data from Phase-Equilibrium Experiments and Natural Pelitic Assemblages. *Contributions to Mineralogy and Petrology*, 143(6): 706–732. https://doi.org/10.1007/s00410-002-0373-6

Pattison, D. R. M., 1992. Stability of Andalusite and Sillimanite and the Al_2SiO_5 Triple Point: Constraints from the Ballachulish Aureole, Scotland. *The Journal of Geology*, 100(4): 423–446. https://doi.org/10.1086/629596

Perchuk, L. L., Lavrent'eva, I. V., 1983. Experimental Investigation of Exchange Equilibria in the System Cordierite-Garnet-Biotite. In: Saxena, S. K., ed., Kinetics and Equilibrium in Mineral Reactions. Springer-Verlag, New York. 199–239

Powell, R., Holland, T. J. B., Worley, B., 1998. Calculating Phase Diagrams Involving Solid Solutions via Non-Linear Equations, with Examples Using THERMOCALC. *Journal of Metamorphic Geology*, 16(4): 577–588. https://doi.org/10.1111/j.1525-1314.1998.00157.x

Ríos, C., García, C., Takasu, A., 2003. Tectono-Metamorphic Evolution of the Silgará Formation Metamorphic Rocks in the Southwestern Santander Massif, Colombian Andes. *Journal of South American Earth Sciences*, 16(2): 133–154. https://doi.org/10.1016/s0895-9811(03)00025-7

Şengün, F., Zack, T., 2016. Trace Element Composition of Rutile and Zr-in-Rutile Thermometry in Meta-Ophiolitic Rocks from the Kazdağ Massif, NW Turkey. *Mineralogy and Petrology*, 110(4): 547–560

Spear, F. S., Selverstone, J., Hickmott, D., et al., 1984. *P-T* Paths from Garnet Zoning: A New Technique for Deciphering Tectonic Processes in Crystalline Terranes. *Geology*, 12(2): 87–90. https://doi.org/10.1130/0091-7613(1984)12<87:ppfgza>2.0.co;2

Stephenson, B. J., Waters, D. J., Searle, M. P., 2000. Inverted Metamorphism and the Main Central Thrust: Field Relations and Thermobarometric Constraints from the Kishtwar Window, NW Indian Himalaya. *Journal of Metamorphic Geology*, 18(5): 571–590. https://doi.org/10.1046/j.1525-1314.2000.00277.x

Tomkins, H. S., Powell, R., Ellis, D. J., 2007. The Pressure Dependence of the Zirconium-in-Rutile Thermometer. *Journal of Metamorphic Geology*, 25(6): 703–713. https://doi.org/10.1111/j.1525-1314.2007.00724.x

Vannay, J.-C., Grasemann, B., 1998. Inverted Metamorphism in the High Himalaya of Himachal Pradesh (NW India): Phase Equilibria versus Thermometry. *Schweizerische Mineralogische und Petrographische Mitteilungen*, 78: 107−132

Weller, O. M., St-Onge, M. R., Waters, D. J., et al., 2013. Quantifying Barrovian Metamorphism in the Danba Structural Culmination of Eastern Tibet. *Journal of Metamorphic Geology*, 31(9): 909–935. https://doi.org/10.1111/jmg.12050

Whitney, D. L., Evans, B. W., 2010. Abbreviations for Names of Rock-Forming Minerals. *American Mineralogist*, 95(1): 185–187. https://doi.org/10.2138/am.2010.3371

Whitney, D. L., Mechum, T. A., Kuehner, S. M., et al., 1996. Progressive Metamorphism of Pelitic Rocks from Protolith to Granulite Facies, Dutchess County, New York, USA: Constraints on the Timing of Fluid Infiltration during Regional Metamorphism. *Journal of Metamorphic Geology*, 14(2): 163–181. https://doi.org/10.1046/j.1525-1314.1996.05836.x

Wu, C.-M., 2015. Revised Empirical Garnet-Biotite-Muscovite-Plagioclase Geobarometer in Metapelites. *Journal of Metamorphic Geology*, 33(2): 167–176. https://doi.org/10.1111/jmg.12115

Wu, C.-M., 2017. Calibration of the Garnet-Biotite-Al_2SiO_5-Quartz Geobarometer for Metapelites. *Journal of Metamorphic Geology*, 35(9): 983–998

Wu, C.-M., Cheng, B. H., 2006. Valid Garnet-Biotite (GB) Geothermometry and Garnet-Aluminum Silicate-Plagioclase-Quartz (GASP) Geobarometry in Metapelitic Rocks. *Lithos*, 89(1/2): 1–23. https://doi.org/10.1016/j.lithos.2005.09.002

Wu, C.-M., Wang, X. S., Yang, C. H., et al., 2002. Empirical Garnet-Muscovite Geothermometry in Metapelites. *Lithos*, 62(1/2): 1–13. https://doi.org/10.1016/s0024-4937(02)00096-8

Wu, C.-M., Zhao, G. C., 2006a. Recalibration of the Garnet-Muscovite (GM) Geothermometer and the Garnet-Muscovite-Plagioclase-Quartz (GMPQ) Geobarometer for Metapelitic Assemblages. *Journal of Petrology*, 47(12): 2357–2368. https://doi.org/10.1093/petrology/egl047

Wu, C.-M., Zhao, G. C., 2006b. The Applicability of the GRIPS Geobarometry in Metapelitic Assemblages. *Journal of Metamorphic Geology*, 24(4): 297–307. https://doi.org/10.1111/j.1525-1314.2006.00638.x

You, Z. D., Han, Y. J., Suo, S. T., et al., 1993. Metamorphic History and Tectonic Evolution of the Qinling Complex, Eastern Qinling Mountains, China. *Journal of Metamorphic Geology*, 11(4): 549–560. https://doi.org/10.1111/j.1525-1314.1993.tb00171.x

Zhang, J., Zhao, G. C., Li, S. Z., et al., 2009. Polyphase Deformation of the Fuping Complex, Trans-North China Orogen: Structures, SHRIMP U-Pb Zircon Ages and Tectonic Implications. *Journal of Structural Geology*, 31(2): 177–193. https://doi.org/10.1016/j.jsg.2008.11.008

Zhang, J., Zhao, G. C., Li, S. Z., et al., 2012. Structural Pattern of the Wutai Complex and Its Constraints on the Tectonic Framework of the Trans-North China Orogen. *Precambrian Research*, 222/223: 212–229. https://doi.org/10.1016/j.precamres.2011.08.009

Zwart, H. J., 1962. On the Determination of Polymetamorphic Mineral Associations, and Its Application to the Bosost Area (Central Pyrenees). *Geologische Rundschau*, 52(1): 38–65. https://doi.org/10.1007/bf01840064